Programmable adhesion through triangular and hierarchical cuts in metamaterial adhesives

Dohgyu Hwang, 1,2,† Chanhong Lee, 1,† and Michael D.Bartlett 1,2*

 $^1\mathrm{Mechanical}$ Engineering, Soft Materials and Structures Lab, Virginia Tech, Blacksburg, VA $24061,\,\mathrm{USA}.$

²Macromolecules Innovation Institute, Virginia Tech, Blacksburg, VA 24061, USA.

†These authors contributed equally to this work *To whom correspondence should be addressed: mbartlett@vt.edu

Cite this article: Dohgyu Hwang, Chanhong Lee, and Michael D. Bartlett. Programmable adhesion through triangular and hierarchical cuts in metamaterial adhesives. *Philosophical Transactions A* 382.2283 (2024): 20240011.

This version of the article has been accepted for publication, after peer review (when applicable) but is not the Version of Record and does not reflect post-acceptance improvements, or any corrections.

The Version of Record is available online at:

https://royalsocietypublishing.org/doi/10.1098/rsta.2024.0011

Abstract

Metamaterial design approaches, which integrate structural elements into material systems, enable the control of uncommon behaviors by decoupling local and global properties. Leveraging this conceptual framework, metamaterial adhesives incorporate non-linear cut architectures into adhesive films to achieve unique combinations of adhesion capacity, release, and spatial tunability by controlling how cracks propagate forward and in reverse directions during separation. Here, metamaterial adhesive designs are explored with triangular cut features while integrating hierarchical and secondary cut patterns among primary nonlinear cuts. Both cut geometry and secondary cut features tune adhesive force capacity and energy of separation. Importantly, the size and spacing of cut features must be designed around a critical length scale. When secondary cut features are greater than a critical length, then cracks can be steered in multiple directions, going both forward and backwards within a primary attachment element. This control over crack dynamics enhances the work of separation by 1.5x while maintaining the peel force relative to a primary cut. If hierarchical cut features are too small or too compliant, they interact and do not distinctly modify crack behavior. This work highlights the importance of adhesive length scales and stiffness for crack control and attachment characteristics in adhesive films.

1 Introduction

The control of adhesion and release is critical for many applications, including diverse fields ranging from manufacturing, electronic packaging, and robotics to wound management, construction, and consumer products.^{1–6} Key adhesive attributes to enable such applications include the ability to resist crack propagation for high adhesion capacity while promoting crack propagation to enable release for recycling, object handling, and surface damage control.⁷ This control of crack dynamics often requires anisotropy in the system, where programmed adhesive properties in different directions can facilitate control of bonding and separation. Typically, adhesives face a trade-off between strong attachment and reversibility, making it challenging to achieve both robust adhesion and easy release.^{8,9} To overcome this limitation, strategies such as tuning interfacial chemistry or incorporating surface features can be used.^{10–12} Additionally, utilizing dynamic materials at the interface can allow for switchable adhesives, where the adhesive can be switched from a low to high adhesive state through a prescribed trigger.^{13,14} However, it may not always be possible to control the trigger for activating adhesion or release, which can limit adhesion tunability to be functional in only specific conditions.

To address these key issues, many works on creating reversible adhesives are focused on controlling the contact geometry or the elastic properties of adhesive materials. For example, micropillars with various geometries and aspect ratios can be patterned on the adhesive layer to tune adhesion strength and toughness. ^{15–21} Controlling adhesive geometry or stiffness also tunes crack dynamics and adhesion performance. This is often achieved through nano- to micron-scale surface features, passive variations of modulus with embedded micro-channels or stiffening components, or actively, for instance, through pneumatic systems that enable adhesive switching. ^{17,18,22,23} At larger length scales, tuning contact stiffness to control adhesion can be achieved by integrating stiff yet flexible fabrics into elastomeric adhesives. ^{22,24} Patterning elasticity by spatially integrating stiff components can also allow

for enhanced adhesion, where changes in adhesive stiffness can dictate crack propagation.^{25–28} Adding incisions in films and substrates can serve a similar function,^{29–34} which can blunt and trap cracks to control adhesion.

An alternative approach to introduce anisotropy into adhesives is to leverage techniques from metamaterial design. Linear cuts in adhesive films can enhance adhesion capacity by 10x while also enabling adhesion to deformable substrates. 31,32 Recently, we demonstrated a strategy that provides strong and reversible adhesion, featuring directional and anisotropic adhesive strength that can be selectively programmed within adhesive films through nonlinear cut architectures or polygonal shapes.³⁵ When peeled in one direction with a high global peel angle, these nonlinear cuts trap and reverse crack propagation by decoupling the global input into a local adhesive response (i.e., low local peel angle). The metamaterial adhesive shows significantly enhanced adhesion on the order of 60x compared to the same material without cuts, while enabling normal crack propagation for low adhesion when peeled in the opposite direction. When utilized in intrinsically strong acrylic adhesive layers, adhesion capacity and adhesion toughness can be further increased to over 3000 N/m (J/m^2) . Notably, these very strong metamaterial adhesives maintain directionality and reuseability. While these metamaterial adhesives exhibited compelling performance across diverse materials, surfaces, and environments, the crack behavior has primarily focused on distinct nonlinear cut designs spaced apart above a characteristic length.³⁵ Additionally, the combination of microarchitectures and macroscopic nonlinear cut architectures can achieve conformal attachment and simultaneous crack trapping across multiple scales for high capacity, programmable release, and reusability.³⁶ However, the impact of altering the macroscale crack path, for example, by the addition of sub-patterns and hierarchy within the nonlinear cut architectures was not examined in our previous work. The incorporation of additional cut features into metamaterial adhesives has the potential to broaden design possibilities and applications by increasing adhesion control through systematic cut structures.

Here, we explore metamaterial adhesives through a systematic investigation of nonlinear

cut geometry and the role of interacting cuts with hierarchical cut structures. For discrete cut features, we focus on triangular cut geometries, where we find that the interior angle of the triangular cut plays a dramatic role in adhesive capacity and anisotropy. When cuts are utilized in hierarchical structures, we find that the interaction between cuts can tune the adhesive capacity as well as the energy required to release the adhesive film. While metamaterial adhesives do not rely on specific chemistry, the choice of adhesive material and backing stiffness can alter the characteristic length scale for design, making material choice a control parameter for the size scale of cut features. This work provides insights into the interplay between nonlinear cut regions, neighboring sub-patterns, and material properties and geometry, and how these aspects influence crack behavior and adhesion characteristics.

2 Results and Discussion

2.1 Anisotropic Adhesion

The metamaterial adhesive consists of an adhesive layer with an inextensible polyethylene terephthalate (PET) backing. We will focus on two different adhesives layers in this work with different adhesive fracture energies, G_c . For low adhesion, we used an elastic polydimethylsiloxane PDMS film (Sylard 184, $G_c = 2.8 \text{ J/m}^2$) and for high adhesion, we used a viscoelastic acrylic film (3M VHB, $G_c = 590 \text{ J/m}^2$). By incorporating triangular cut patterns into the adhesive film, the metamaterial adhesive is designed to achieve high adhesion and easy release simultaneously in opposite peel directions within a single film (Fig. 1a). We define the max-state as the condition where strong adhesion is achieved and the min-state as the condition where easy release is achieved. High adhesion is attained in the max-state direction by guiding cracks along the interconnects, arresting them at the tips, and forcing them to reverse their propagation direction.³⁵ Conversely, easy release is enabled in the min-state direction by permitting cracks to propagate forward, a behavior commonly observed in unpatterned adhesives, resulting in an adhesion directionality of ~ 30 for the low G_c

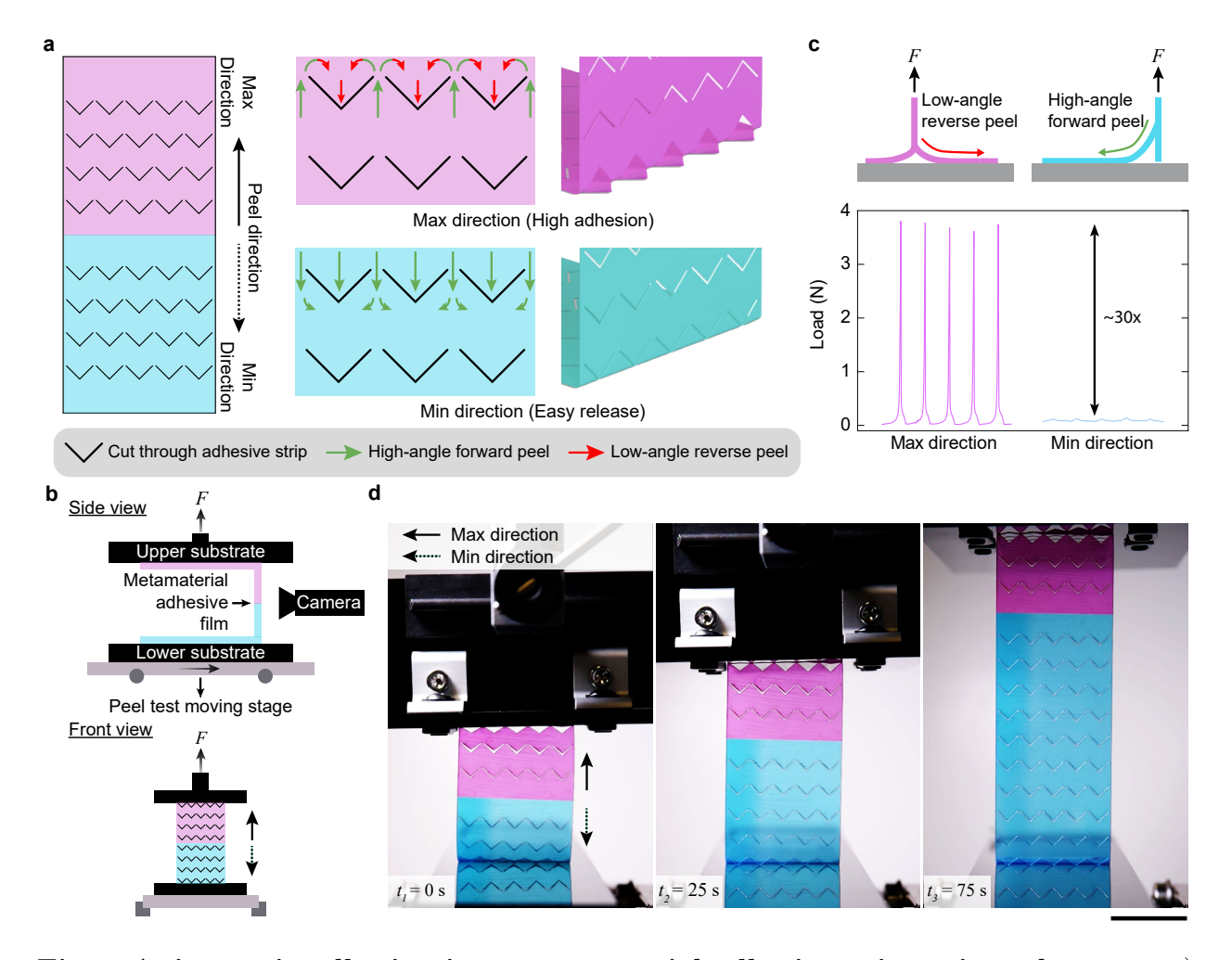


Fig. 1 Anisotropic adhesion in a metamaterial adhesive using triangular cuts. a) High adhesion is achieved when the film is peeled in the max-state direction by trapping the cracks and forcing them to reverse direction (red arrows) to propagate backwards. Easy release occurs in the min-state peel direction by allowing for normal forward crack propagation (green arrows). b) Anisotropic adhesion is demonstrated by peeling the metamaterial adhesive from an upper and the lower substrate. c) Peel force curves of the metamaterial adhesive in the max and min peel direction. d) Image sequence showing adhesion anisotropy during the peeling of a metamaterial adhesive with a layout of triangular cuts. Red and blue dyes are added into the adhesive layer for visualization. In Fig 1, $w_{int} = 1$ mm, $N_p = 5$, and the adhesive layer is the low G_c PDMS adhesive.

PDMS adhesive. (Fig. 1c). We illustrate the directional dependence of adhesion and release by reverse crack propagation through a metamaterial adhesive adhered to both an upper and lower substrate and peeling it under 90° (Fig. 1b,d and Supplementary Video 1). The triangular cuts in the adhesive film adhered to the upper substrate undergo reverse crack propagation, while the film adhered to the lower substrate undergoes normal forward crack

propagation. Due to this difference in crack propagation behavior, the adhesive adhered to the upper substrate remains bonded while it is released from the lower substrate, highlighting the ability to tune adhesion and release capacity through nonlinear cut architectures.

2.2 Properties of metamaterial adhesive with varying triangular cuts

To achieve optimal adhesion and release using nonlinear cuts, it is essential to carefully design the shapes and dimensions of the cut patterns for a given set of materials. Unlike a typical unpatterned adhesive film, which exhibits a linear crack front across its width during peeling, metamaterial adhesives display a complex crack propagation profile. Consequently, adjusting the cut designs influences how effectively nonlinear cuts control crack propagating, ultimately determining adhesion capacity and release. The triangular cut pattern is characterized by its width w_p and its interior angle β (Fig. 2a). Each triangular cut is spaced w_{int} apart within each row, with a distance of s between rows along the peel direction. The total width w of the adhesive remains constant throughout the experiments at w=46 mm.

The interior angle β plays a large role in determining the crack behavior and the adhesion enhancement as seen for the low G_c elastic PDMS adhesive Fig. 2b and high G_c viscoelastic acrylic adhesive in Fig. S1. When β is equal to zero, the cut is a straight line, creating alternating stiff and compliant regions perpendicular to the width of the adhesive film. As the crack line reaches the compliant region, it splits along each interconnect defined by the linear cuts. Further loading arrests the crack at the tips that connect a stiff region, the max-state adhesive strength (F_{max}) enhances when the crack travels into the stiff region, followed by a sudden interfacial failure. As β is increased, the linear cut transitions to the onset of a non-linear triangular cut pattern. At this point, reverse crack propagation begins to occur and F_{max} increases. Notably, once β reaches 45-60°, F_{max} saturates and the geometry achieves optimized adhesion enhancement similar to that exhibited by a triangular pattern with β of 75° and a rectangular pattern $(\beta = 90^{\circ})$. In this case, the rectangle with $\beta = 90^{\circ}$

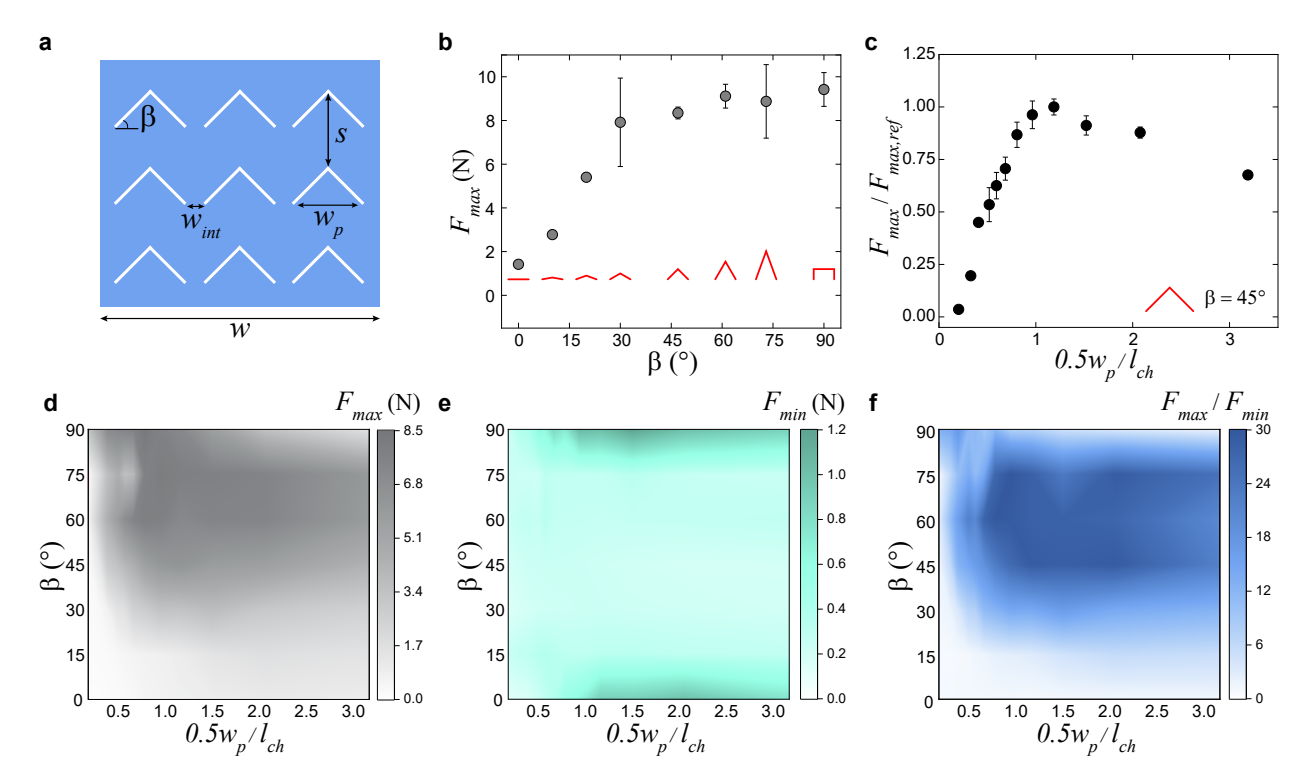


Fig. 2 Properties of metamaterial adhesive with varying triangular cuts. a) Schematic diagram with relevant geometry of a metamaterial adhesive consisting of triangular patterns. b) Max-state peak force values F_{max} as a function of the prescribed angle β of triangular patterns. (Note that $\beta=0^{\circ}$ and $\beta=90^{\circ}$ corresponds to linear and rectangular patterns, respectively.) c) Normalized peak force $(F_{max}/F_{max,ref})$ of triangular patterns $(\beta=45^{\circ})$ as a function of the dimensionless geometric parameter $0.5w_p/l_{ch}$. The reference peak force $(F_{max,ref})$ denotes the highest F_{max} for a given $0.5w_p/l_{ch}$ data set,and $l_{ch}=3.0$ mm for this adhesive system. d-f) Max-state peak force F_{max} , min-state peak force F_{min} , and adhesion directionality F_{max}/F_{min} of a collection of linear, triangular, and rectangular patterns with varying angles and dimensionless geometric parameters, respectively. In Fig 2, $w_{int}=1$ mm and $N_p=7$, and the adhesive layer is the low G_c PDMS adhesive.

was selected to have a height of $w_p/2$, having equal height to a triangle with $\beta = 45^{\circ}$.

The cut width w_p is also important for achieving optimized adhesion enhancement (Fig. 2c). When w_p is changed for a given β of 45° with other dimensions fixed, the maximum force (F_{max}) initially increases as $0.5w_p$ increases and then reaches a peak at a characteristic value. This is plotted in Fig. 2c as $F_{max}/F_{max,ref}$, where $F_{max,ref}$ denotes the highest F_{max} for a given $0.5w_p/l_{ch}$ data set. The underlying mechanism involves transitioning between two distinct phases in reverse crack propagation. When $0.5w_p$ falls below a characteristic length l_{ch} , cracks from adjacent interconnect tips merge prior to reaching F_{max} , leading to a diminished

force capacity. When $0.5w_p$ is roughly equal to l_{ch} , cracks originating from neighboring interconnect tips do not intersect, resulting in circular delamination regions centered at each interconnect tip and achieving optimum adhesion force. The characteristic length is given by:

$$l_{ch} = \sqrt{\frac{2D}{G_c} \frac{w_{int}}{w} (N_p^* + 1)}$$
 (2.1)

where G_c is the critical energy release rate, experimentally determined by peeling an unpatterned adhesive strip (See Experimental section), D is the flexural rigidity of the adhesive film, w is the total adhesive width, w_{int} is the width of an interconnect, and N_p^* is the optimal number of cut patterns for achieving the highest F_{max} . N_p^* can be determined either experimentally (i.e., the number of cut patterns that shows the highest F_{max}) or calculated (see Supplementary Information in reference 35). The PDMS/PET film gives $l_{ch} = 3.0$ mm. As $0.5w_p$ increases further, the adhesive force that peaks at the characteristic value decreases. Although the cut geometry that exceeds the characteristic length achieves optimal adhesive capacity at the level of each interconnect tip, a large w_p limits the number of cut patterns for a given total width w of the film. This results in a reduced number of individually optimum cut patterns and diminished adhesive capacity.

To establish a design principle for metamaterial adhesives, we assess adhesion performance in both the max and min peel directions across a wide range of β and w_p values for cut patterns. The optimum adhesion force in the max state (F_{max}) is achieved when both conditions $\beta \geq 60^{\circ}$ and $0.5w_p/l_{ch} \approx 1$ are satisfied (Fig. 2d). The observation aligns with the findings in Fig. 2b, suggesting that triangular cut features perform similarly to rectangular cut features when $\beta \geq 60^{\circ}$. This similarity can be attributed to the fact that the centroid of an isosceles triangle approaches the centroid of a rectangle of the same width for $\beta \approx 70^{\circ}$, resulting in similar bending rigidity. When either $\beta \leq 30^{\circ}$ or $0.5w_p/l_{ch} \ll 1$, the adhesive strength is notably reduced, and in both cases, effective reverse crack propagation does not occur.

In the min peel directions, the optimum adhesive force (F_{min}) is achieved across an entire set of triangular patterns $(15^{\circ} \leq \beta \leq 75^{\circ})$ (Fig. 2e). The value is comparable to the steady-state adhesive strength of the unpatterned adhesive film, attributed to negligible crack arresting in the vicinity of interconnect regions during normal forward crack propagation. F_{min} is notably increased under two conditions: $\beta = 0^{\circ}$ with $0.5w_p/l_{ch} \geq 1$ and $\beta = 90^{\circ}$ with $0.5w_p/l_{ch} \geq 1$. Both linear $(\beta = 0^{\circ})$ and rectangular $(\beta = 90^{\circ})$ patterns have cuts perpendicular to the peel direction, resulting in alternating stiff and compliant regions. When the crack front crosses the stiff interface, it can be temporarily trapped, leading to increased bending rigidity and contact width, which suppresses release capability.³¹

To determine the combinations of β and w_p that achieve the highest adhesion directionality, we compute F_{max}/F_{min} and find a ratio of 30 when both conditions $45^{\circ} \leq \beta \leq 75^{\circ}$ and $0.5w_p/l_{ch} \approx 1$ are met (Fig. 2f). These conditions also maintain high F_{max} , similar to metamaterial adhesives with rectangular cuts, while enabling F_{min} to approach the level of an unpatterned adhesive film.

2.3 Effects of hierarchical cut patterns on adhesion

Optimal adhesion enhancement in metamaterial adhesives is achieved through the design of both nonlinear cut architectures and interconnect structures, taking into consideration the characteristic length. When the size of the feature is above l_{ch} the cracks do not merge before reaching F_{max} , resulting in the highest level of adhesion enhancement. These samples exhibit reverse crack propagation and circular delamination around each interconnect tip, showing that the crack path during the peeling of metamaterial adhesives is influenced the cut shape and size. These enhancement mechanism involves the storage of mechanical energy during reverse crack propagation, followed by rapid energy release and complete adhesive delamination. This process leads to a peak in the peel force profile. During peeling of metamaterial adhesives, the work of separation (W), which corresponds to the area under the force-displacement curve, will also vary based on design. Consequently, adjusting the

crack dynamics beyond circular delamination centered at interconnect tips can provide an approach to controlling the adhesion capacity and work of separation in a specific adhesive material.

To investigate the effects of hierarchical and secondary cut patterns we created samples that consisted of primary triangular cut features with sub-patterns having dimensions/spacings of size l_{sub} . The w_p of the primary triangle is 5.33 mm and l_{sub} is 0.5 mm. These are arranged as linear cuts (design i, ii, iii, iv) or hierarchical triangular structures (design v, vi, vii) within the primary triangular feature as shown in Figure 3a. Within these geometries, we vary G_c through the adhesive layer and vary the bending rigidity D by changing the thickness of the PET backing layer, with both parameters impacting l_{ch} . We vary these parameters across three combinations such that: $l_{sub} < l_{ch}$ with low G_c and low D. This uses a PDMS adhesive and a 0.07 mm PET layer resulting in $l_{ch} = 3.0$ mm. $l_{sub} < l_{ch}$ with high G_c and high D. This uses a viscoelastic acrylic adhesive and a 0.375 mm PET layer resulting in $l_{ch} = 3.3$ mm. $l_{sub} \simeq l_{ch}$ with high G_c and low D. This uses a viscoelastic acrylic adhesive and a 0.07 mm PET layer resulting in $l_{ch} = 0.44$ mm. The combination of low G_c , and high D is not feasible as l_{ch} is too large. For these geometries, we examine the force profiles (Figure 3b) and work of separation W (Figure 3c) during peeling.

For $l_{sub} < l_{ch}$ with low G_c and low D, for sub-patterns with linear cuts (design, i, ii, iii, iv, vii), or hierarchical features (design v, vi), we find that both F_{max} and W are reduced compared to a pristine triangle reference without the sub-patterns ($F_{triangle}$). The labyrinth-like sub-pattern (design vii) decreases F_{max} and W relative to the other architectures. When examining the peel curves, all of these samples show a single, sharp force peak with a small shoulder after the peak. We attribute this behavior to the interaction between the sub-patterns and the cracks during crack propagation. As seen in Figure 3d and Supplementary Video S2, as the crack front progresses from the base of the primary triangle, the crack moves through the secondary feature without altering the behavior of the initial crack. Therefore, these secondary features are not large enough to deflect the crack which reduces

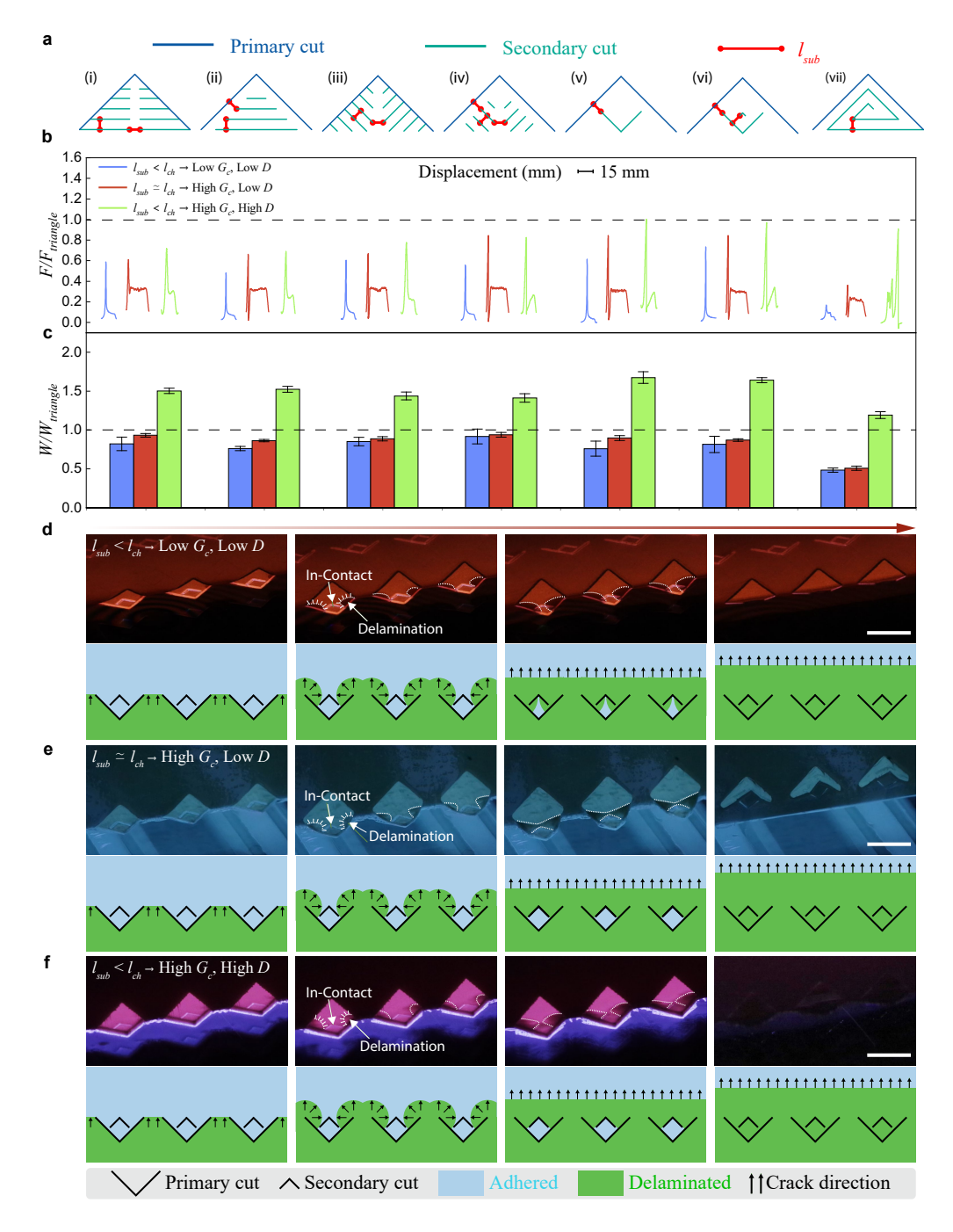


Fig. 3 Effects of sub-patterns and hierarchy on adhesion characteristics. a) Schematics of sub-patterns placed within primary triangular cuts. b) Peel force F normalized by the force of a pristine triangle $(F_{triangle,max})$ as a function of displacement for various sub-patterns for low adhesion, elastic PDMS film (Sylard 184, $G_c = 2.8 \text{ J/m}^2$) and high adhesion, viscoelastic acrylic film (3M VHB, $G_c = 590 \text{ J/m}^2$). c) Normalized work of separation $W/W_{triangle}$ for various sub-patterns. d) Images and schematics of the peel front for the peeling of pattern v when $l_{sub} < l_{ch}$ with a PDMS film and e) when $l_{sub} > l_{ch}$ with a 3M VHB film. Scale bar is 5 mm. In Fig 3, $w_{int} = 2 \text{ mm}$ and $N_p = 6$.

the effectiveness of the crack arresting behavior. Although reverse crack propagation is maintained through the primary triangular feature, without additional crack deflection and with a low bending rigidity, adhesion is reduced relative to pristine features.

For $l_{sub} \simeq l_{ch}$ with high G_c and low D, we find that F_{max} and W are reduced compared to a pristine reference without sub-patterns ($F_{triangle}$). The peel curves also show a single sharp peak during reverse crack propagation, but due to the high G_c a force plateau is observed in the area between cut patterns which then decreases as the crack moves through the interconnects and approaches the next cut pattern. When examining the crack propagation behavior for $l_{sub} \simeq l_{ch}$ pattern v, once the crack arrests at the interconnect tips, it begins to propagate inward. However, it does not just propagate through the sub-pattern, but instead is arrested and then must reverse direction again to fully delaminate the film (Figure 3e and and Supplementary Video 2). However, with the lower bending rigidity D of the film the redirection of the crack does not strongly influence the force profile, which is why W stays consistent in the presence of the secondary patterns.

For $l_{sub} < l_{ch}$ with high G_c and high D (design, i, ii, iii, iv), we find that the peel curves show a peak and then a coupled shoulder. For hierarchical features (design v, vi) we see a sharp peak, a decrease, then an increasing force again in the area between cut patterns. While F_{max} still decreases for design, i, ii, iii, iv, vii, due to the shoulder after the primary peak, W increases compared to the pristine sample. For hierarchical features (design v, vi), $F_{max} \approx F_{triangle}$, while W has increased by 1.5x compared to the pristine sample. When examining the debonding process for $l_{sub} < l_{ch}$ with high G_c and high D, we see that film does not bend as readily as it did for the low D films (Figure 3f and Supplementary Video 2). Although $l_{sub} < l_{ch}$, the increased bending rigidity requires more energy to debond which broadens the force profile as the cracks move through the secondary features and increases W. These results highlight the importance of considering both l_{ch} and D for the design of sub-patterns and primary patterns in metamaterial adhesives.

The performance of metamaterial adhesive films is impacted by sub-patterns. Figure 4a

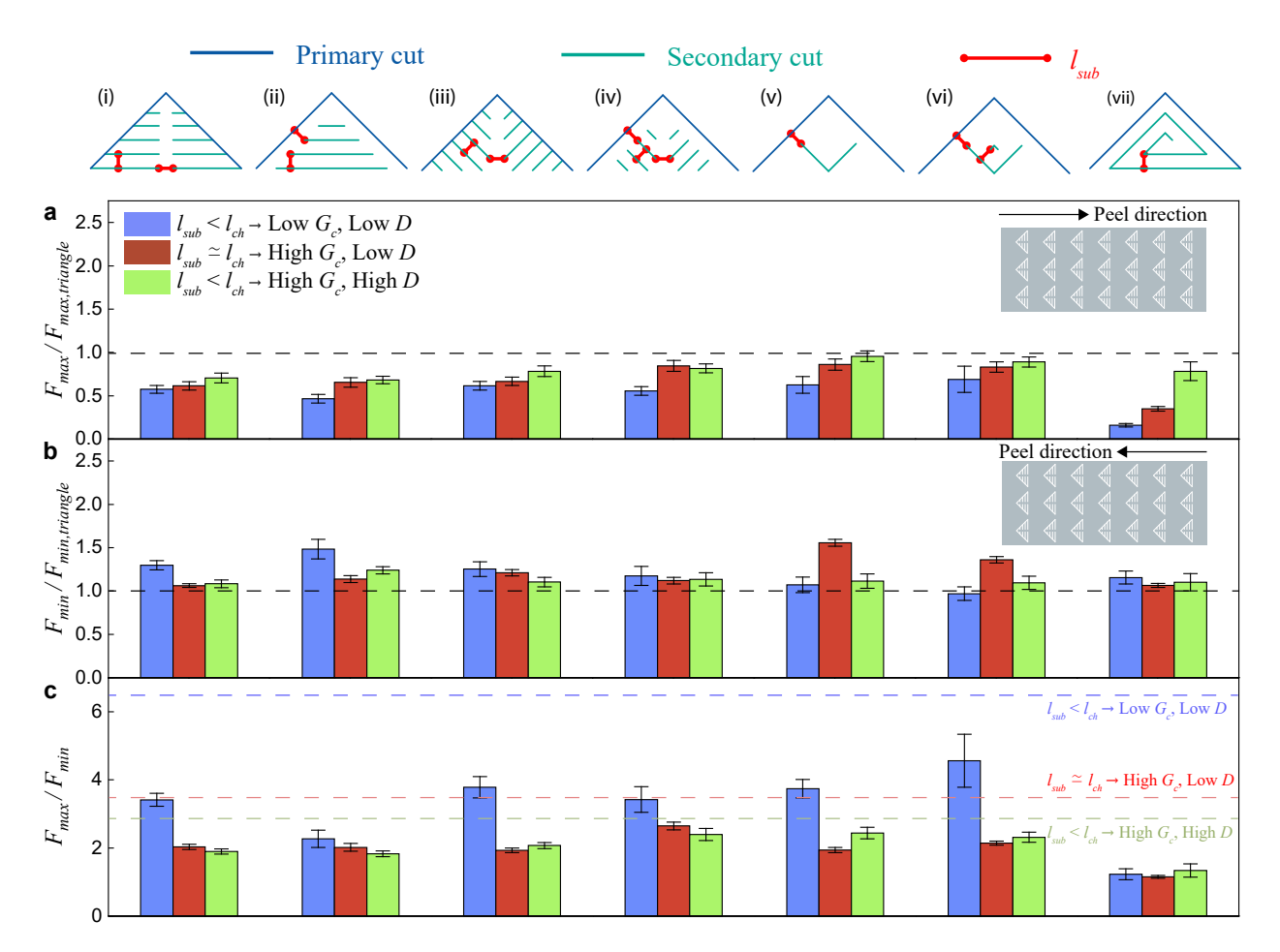


Fig. 4 Performance of sub-patterns and hierarchy on adhesion characteristics. a) The F_{max} enhancement ratio $(F_{max}/F_{max,triangle})$ of triangular cut and hierarchical architectures. b) The F_{min} enhancement ratio $(F_{min}/F_{min,triangle})$ of triangular cut and hierarchical architectures. c) The adhesion directionality F_{max}/F_{min} of triangular cut and hierarchical architectures. The blue dashed line for $l_{sub} < l_{ch}$ and the red dashed line for $l_{sub} > l_{ch}$ represent the pristine triangle directionality for each material. In Fig 4, $w_{int} = 2$ mm and $N_p = 6$.

summarizes the F_{max} enhancement ratio ($F_{max}/F_{max,triangle}$). The results indicate that in all cases examined in this work a pristine cut feature shows a larger F_{max} than a cut feature with sub-patterns. Designs v and vi show the highest F_{max} , which we attribute to the sub-pattern being spaced as far as possible from the interconnect. This spacing allows the force to develop before the crack reaches a sub-pattern during the initial crack growth at the interconnect tip. Figure 4b summarizes the F_{min} ratio ($F_{min}/F_{min,triangle}$). The results show that the sub-patterns examined in this work increase the release force F_{min} . Figure 4c summarizes

the adhesion directionality F_{max}/F_{min} . As the sub-patterns tend to generally decreases F_{max} and increase F_{min} , the adhesion directionality is reduced by adding sub-patterns relative to a pristine cut feature. We note that designs v and vi show the most promising adhesion directionality compared to pristine cut features.

3 Conclusion

In this work, we show that in metamaterial adhesives both the geometry of primary nonlinear cut patterns and sub-patterns, along with material properties and film thickness, play significant roles in influencing crack propagation behavior and, consequently, the resulting adhesion performance. Carefully designed triangular patterns provide tunable adhesion enhancement and directionality, offering a distinct functionality not attained by linear cut patterns or unpatterned adhesives. Further, sub-patterns must be designed around the characteristic adhesive length scale, l_{ch} , and bending rigidity D. When the sub-pattern cuts or spacing are smaller than l_{ch} , they tend to decrease removal force and energy. However, sub-patterns within films with higher bending rigidity can maintain removal forces while enhancing the energy of separation by up to 1.5x. This points to the importance of cut design and material choice for metamaterial adhesives, especially when secondary cut patterns or hierarchical features are incorporated. As such, these metamaterial adhesives can serve as a versatile design strategy for controlling crack propagation and enhancing adhesion performance across various applications and materials.

4 Experimental

Adhesive Fabrication

PET films (McMaster-Carr, $E=2.6\pm0.1$ GPa) are patterned by laser cutting (Universal Laser VLS4.60 Laser System 75W CO₂). A thin PDMS layer (Sylgard 184, 20:1 base resin-

to-crosslinker ratio; $E=880\pm40$ kPa, $t_{PDMS}\approx120~\mu\mathrm{m}$) was then created on a glass plate using a thin film applicator (ZUA 2000; Zehntner Testing Instruments) and cured at 80°C for 60 min. Another thin layer of PDMS with the same mixing ratio was poured onto the cured PDMS layer using a thin film applicator ($t_{PDMS}\approx30~\mu\mathrm{m}$). We treated the cut PET films with oxygen plasma (pressure : 300 mTorr, 3 min), attached them onto the uncured PDMS prepolymer, and cured the composite at 80°C for 60 min. VHB adhesives were made with 125 $\mu\mathrm{m}$ VHB and PET films (McMaster-Carr, E=2.6. They were laminated together with a roller and then patterned by laser cutting (Universal Laser VLS4.60 Laser System 75W CO₂).

Adhesive Characterization

We used a 90 ° peel test setup to measure the adhesion strength between an adhesive strip and an acrylic substrate using an Instron 5944 mechanical tester at a constant displacement rate of 1 mm/s. Before each run, the surface of each specimen was cleaned with isopropyl alcohol and tape to remove residues. The adhesive strip was then placed on an acrylic substrate with a rubber roller. A dwell time of 3 min was kept constant before performing each peel test. The critical energy release rate G_c of the adhesive was obtained by calculating the plateau force of an unpatterned adhesive strip. We calculate the work of separation W, which is the work done by external loading to separate the adhesive from the substrate per unit area, $\frac{1}{w(\delta_p - \delta_0)} \int_{\delta_0}^{\delta_p} F(\delta) d\delta$. We take δ_0 as the displacement where a reverse crack propagation starts and δ_p as the length of the cut pattern repeat unit s.

Acknowledgment

We acknowledge support from the National Science Foundation under the DMREF program (award number: 2119105).

Data

Data underlying this manuscript are made accessible through the https://data.lib.vt.edu/Virginia Tech Data Repository at https://doi.org/10.7294/26659882https://doi.org/10.7294/26659882 37

References

- [1] Mica Grujicic, Vijay Sellappan, Mohammed A. Omar, Norbert Seyr, Andreas Obieglo, Marc Erdmann, and Jochen Holzleitner. An overview of the polymer-to-metal directadhesion hybrid technologies for load-bearing automotive components. J. Mater. Process. Technol., 197(1):363–373, 2008.
- [2] Byungsuk Yoo, Sungbum Cho, Seungwan Seo, and Jongho Lee. Elastomeric angled microflaps with reversible adhesion for transfer-printing semiconductor membranes onto dry surfaces. ACS Appl. Mater. Interfaces, 6(21):19247–19253, 2014.
- [3] Xiang Dai, Mark V. Brillhart, and Paul S. Ho. Adhesion measurement for electronic packaging applications using double cantilever beam method. *IEEE Trans. Components Packag. Technol.*, 23(1):101–116, 2000.
- [4] Allen R. Hutchinson and Stefan Iglauer. Adhesion of construction sealants to polymer foam backer rod used in building construction. *Int. J. Adhes. Adhes.*, 26(7):555–566, 2006.
- [5] Alborz Mahdavi, Lino Ferreira, Cathryn Sundback, Jason W Nichol, Edwin P Chan, David JD Carter, Chris J Bettinger, Siamrut Patanavanich, Loice Chignozha, Eli Ben-Joseph, Alex Galakatos, Howard Pryor, Irina Pomerantseva, Peter T. Masiakos, William Faquin, Andreas Zumbuehl, Seungpyo Hong, Jeffrey Borenstein, Joseph Vacanti, Robert Langer, and Jeffrey M. Karp. A biodegradable and biocompatible gecko-inspired tissue adhesive. Proceedings of the National Academy of Sciences, 105(7):2307–2312, 2008.

- [6] Li Liu, Kristina Kuffel, Dylan K Scott, Gabriela Constantinescu, Hyun-Joong Chung, and Jana Rieger. Silicone-based adhesives for long-term skin application: Cleaning protocols and their effect on peel strength. Biomedical Physics & Engineering Express, 4(1):015004, 2017.
- [7] Costantino Creton. Pressure-Sensitive Adhesives: An Introductory Course. MRS Bull., 28(06):434–439, 2003.
- [8] Yichao Tang, Qiuting Zhang, Gaojian Lin, and Jie Yin. Switchable adhesion actuator for amphibious climbing soft robot. *Soft robotics*, 5(5):592–600, 2018.
- [9] Michael D Bartlett, Scott W Case, Anthony J Kinloch, and David A Dillard. Peel tests for quantifying adhesion and toughness: A review. Progress in Materials Science, 137:101086, 2023.
- [10] Kenneth R Shull. Contact mechanics and the adhesion of soft solids. *Materials Science* and Engineering: R: Reports, 36(1):1–45, 2002.
- [11] Dirk-M. Drotlef, Morteza Amjadi, Muhammad Yunusa, and Metin Sitti. Bioinspired Composite Microfibers for Skin Adhesion and Signal Amplification of Wearable Sensors. Adv. Mater., 1701353:1701353, 2017.
- [12] Sangyul Baik, Da Wan Kim, Youngjin Park, Tae-Jin Lee, Suk Ho Bhang, and Changhyun Pang. A wet-tolerant adhesive patch inspired by protuberances in suction cups of octopi. *Nature*, 546(7658):396–400, 2017.
- [13] Vito Cacucciolo, Herbert Shea, and Giuseppe Carbone. Peeling in electroadhesion soft grippers. *Extreme Mechanics Letters*, 50:101529, 2022.
- [14] Andrew B Croll, Nasibeh Hosseini, and Michael D Bartlett. Switchable adhesives for multifunctional interfaces. *Advanced Materials Technologies*, 4(8):1900193, 2019.

- [15] Hoon Eui Jeong, Jin-Kwan Lee, Hong Nam Kim, Sang Heup Moon, and Kahp Y Suh. A nontransferring dry adhesive with hierarchical polymer nanohairs. *Proceedings of the National Academy of Sciences*, 106(14):5639–5644, 2009.
- [16] Nicholas J Glassmaker, Anand Jagota, Chung-Yuen Hui, William L Noderer, and Manoj K Chaudhury. Biologically inspired crack trapping for enhanced adhesion. *Proc.* Natl. Acad. Sci. U. S. A., 104(26):10786–10791, 2007.
- [17] Yiğit Mengüç, Sang Yoon Yang, Seok Kim, John A. Rogers, and Metin Sitti. Gecko-Inspired Controllable Adhesive Structures Applied to Micromanipulation. Adv. Funct. Mater., 22(6):1246–1254, jan 2012.
- [18] Liehui Ge, Sunny Sethi, Lijie Ci, Pulickel M Ajayan, and Ali Dhinojwala. Carbon nanotube-based synthetic gecko tapes. Proceedings of the National Academy of Sciences, 104(26):10792–10795, 2007.
- [19] Kellar Autumn and Nick Gravish. Gecko adhesion: evolutionary nanotechnology. *Philos. Trans. R. Soc. A Math. Phys. Eng. Sci.*, 366(1870):1575–1590, 2008.
- [20] Liangti Qu, Liming Dai, Morley Stone, Zhenhai Xia, and Zhong Lin Wang. Carbon nanotube arrays with strong shear binding-on and easy normal lifting-off. Science (80-.)., 322:238–242, 2008.
- [21] Seok Kim, Jian Wu, Andrew Carlson, Sung Hun Jin, Anton Kovalsky, Paul Glass, Zhuangjian Liu, Numair Ahmed, Steven L Elgan, Weiqiu Chen, Placid M. Ferreira, Metin Sitti, and John A. Huang, Yonggang Rogers. Microstructured elastomeric surfaces with reversible adhesion and examples of their use in deterministic assembly by transfer printing. Proceedings of the National Academy of Sciences, 107(40):17095–17100, 2010.
- [22] Michael D. Bartlett, Andrew B. Croll, Daniel R. King, Beth M. Paret, Duncan J. Irschick, and Alfred J. Crosby. Looking beyond fibrillar features to scale gecko-like adhesion. Adv. Mater., 24(8):1078–1083, 2012.

- [23] Abhijit Majumder, Animangsu Ghatak, and Ashutosh Sharma. Microfluidic adhesion induced by subsurface microstructures. *Science*, 318(5848):258–261, 2007.
- [24] Daniel R King, Michael D Bartlett, Casey A Gilman, Duncan J Irschick, and Alfred J Crosby. Creating gecko-like adhesives for "real world" surfaces. Adv. Mater., 26(25):4345–4351, 2014.
- [25] Shuman Xia, Laurent Ponson, Guruswami Ravichandran, and Kaushik Bhattacharya. Toughening and asymmetry in peeling of heterogeneous adhesives. *Phys. Rev. Lett.*, 108(19):1–5, 2012.
- [26] Shuman Xia, Laurent Ponson, Guruswami Ravichandran, and Kaushik Bhattacharya. Adhesion of heterogeneous thin films - I: Elastic heterogeneity. J. Mech. Phys. Solids, 61(3):838–851, 2013.
- [27] Kevin Kendall. Control of Cracks by Interfaces in Composites. Proc. R. Soc. A Math. Phys. Eng. Sci., 341(1627):409–428, jan 1975.
- [28] Michael D Bartlett and Alfred J Crosby. Material Transfer Controlled by Elastomeric Layer Thickness. *Mater. Horizons*, 1(5):507–512, 2014.
- [29] Jun Young Chung and Manoj K Chaudhury. Roles of discontinuities in bio-inspired adhesive pads. J. R. Soc. Interface, 2(2):55–61, 2005.
- [30] Animangsu Ghatak, L Mahadevan, Jun Young Chung, Manoj K Chaudhury, and Vijay Shenoy. Peeling from a biomimetically patterned thin elastic film. Proc. R. Soc. Lond. A. Math. Phys. Sci., 460(2049):2725–2735, 2004.
- [31] Doh-Gyu Hwang, Katie Trent, and Michael D Bartlett. Kirigami-inspired structures for smart adhesion. ACS applied materials & interfaces, 10(7):6747–6754, 2018.
- [32] Ruike Zhao, Shaoting Lin, Hyunwoo Yuk, and Xuanhe Zhao. Kirigami enhances film adhesion. *Soft Matter*, 14:2515–2525, 2018.

- [33] Qi Li, Weixuan Liu, Canhui Yang, Ping Rao, Pengyu Lv, Huiling Duan, and Wei Hong. Kirigami-inspired adhesion with high directional asymmetry. *Journal of the Mechanics and Physics of Solids*, 169:105053, 2022.
- [34] Haotian Wang, Chen Pan, Haiyuan Zhao, Tingyu Wang, and Yafeng Han. Design of a metamaterial film with excellent conformability and adhesion for bandage substrates. J. Mech. Behav. Biomed. Mater., page 104799, 2021.
- [35] Dohgyu Hwang, Chanhong Lee, Xingwei Yang, Jose M Pérez-González, Jason Finnegan, Bernard Lee, Eric J Markvicka, Rong Long, and Michael D Bartlett. Metamaterial adhesives for programmable adhesion through reverse crack propagation. *Nature Materials*, 22(8):1030–1038, 2023.
- [36] Seongjin Park, Dong Kwan Kang Kang, Donghyuk Lee, Geonjun Choi, Jaeil Kim, Chanhong Lee Lee, Minho Seong, Michael D. Bartlett, and Hoon Eui Jeong. Multiscale crack trapping for programmable adhesives. *Science Advances*, 10.1126/sciadv.adq3438, 2024.
- [37] Dohgyu Hwang, Chanhong Lee, and Michael D. Bartlett. Dataset for programmable adhesion through triangular and hierarchical cuts in metamaterial adhesives. *University Libraries, Virginia Tech. Dataset.*, https://doi.org/10.7294/26659882, 2024.